

# Design stage ray-optical assessments of a composite parabolic trough

R. N. SINGH

Physics Department, Indian Institute of Technology, Delhi, India.

S. S. MATHUR, T. C. KANDPAL

Centre of Energy Studies, Indian Institute of Technology, Delhi, India.

A ray-optical evaluation of the constructional and concentration characteristics of a composite parabolic trough (CPT) with flat receiver is given. The region of non-zero intensity in the focal plane, the intensity in the central solar image and the receiver intercept fraction for a typical CPT are studied and the significance of the results at the design stage is pointed out.

## Introduction

Parabolic trough and bowls are well established concentrators of solar energy and their optical design aspects have been the subject matter of many papers. EVANS [1], and MCDERMID and HORTON [2] in their recent papers have referred to the earlier work in great detail. The common approach used in the fabrication of the trough concentrators is to machine parabolic ribs in a programmed milling machine which are then attached to a torque tube. Preformed aluminium sheets matched to the parabolic shape of the ribs are next bolted on to the ribs to serve as the foundation for the parabolic reflector. However, as discussed by GIUTRONICH [3], inexpensive and large concentrators are invariably made by composing the parabolic shape with the help of many small elementary flat mirrors. In the context of non focussing concentrators, SHAPIRO [4] refers to these as polygonal trough concentrators. In the present paper we give a simple ray-optical analysis, based on the work of COSBY [5] and concerning focussing parabolic trough made from elementary flat mirror strips, referred to as "composite" here and used with a flat receiver. Constructional and concentration characteristics of a typical composite parabolic trough (CPT) obtained in this paper are presented in a graphical form. The usefulness of the results at the design stage of a solar energy system has also been demonstrated.

## Ray-optical analysis

A pictorial representation of a section of the CPT is given in fig. 1a. It consists of  $(2k+1)$  elements of same width  $d$ . The trough aperture, focal length and rim angle are taken to be  $D$ ,  $a$ , and  $\theta$ , respectively. In the analysis we assume perfect tracking,

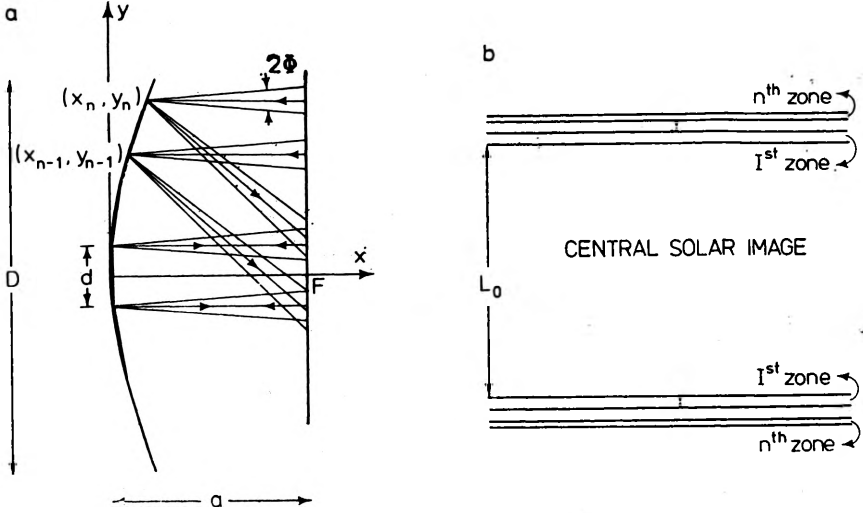


Fig. 1. a) The concentration ray geometry of a CPT, b) Focal plane zones of various intensity levels

uniform solar disc and uniform reflectivity with respect to the angle of incidence and the wavelength over the solar spectrum. Denoting by  $(x_n, y_n)$  and  $(x_{n-1}, y_{n-1})$  the coordinates of the end points of the  $n$ -th flat mirror element, its inclination with the  $y$ -axis is given by

$$\tan \Psi_n = (y_n + y_{n-1})/4a. \quad (1)$$

A cone of solar rays reflected from the  $n$ -th element intersects the receiver plane over a width ( $L_n = |y_n''| + |y_n'|\rangle$ ) such that

$$y_n'' = y_n - (a - x_n) \tan(2\Psi_n - \Phi), \quad (2)$$

and

$$y_n' = y_{n-1} - (a - x_{n-1}) \tan(2\Psi_n + \Phi). \quad (3)$$

From these formulae, the two constructional characteristics, tilt  $\Psi_n$  and receiver plane intercept width  $L_n$ , may be calculated for all the elements in any given case.

Assuming that the incident solar flux, after reflection from CPT, is spread over a width  $L_n$  for the  $n$ -th element, its elemental contribution to intensity may be written in the form

$$CI_n = \frac{pq_s d \cos \Psi_n}{L_n}, \quad (4)$$

where  $p$  is the reflectivity, and  $q_s$  is the incident solar flux. Now elemental contribution of all the mirror elements add up to give the intensity over the width  $L_0$  corresponding to the axial mirror element of the CPT. The intensity in this region of the receiver due to reflection from the CPT becomes

$$I_0(y) = CI_0 + 2 \sum_{n=1}^k CI_n \quad (5)$$

for  $y_0' < y < y_0''$ .

The number of mirror elements contributing to the intensity in the receiver plane diminishes progressively as we move outward from the margin of the central solar image, beginning, of course, with loss of the contribution from the axial mirror element. Thus for zone  $n$  (see fig. 1b) in the receiver plane region beyond the central solar image

$$I_n(y) = I_0(y) - 2 \sum_{n=0}^{n-1} CI_n, \quad (6)$$

for

$$y_{n-1}^u < y < y_n^u, \text{ and } y_n^l < y < y_{n-1}^l.$$

Equation (6) means that the finite sized mirror elements used in the fabrication of the CPT produce zones of various intensity levels. In practice, however, the physical size of a zone is so small compared to the width  $L_0$  of the central solar image, that the intensity of the zone itself may be assigned to its midpoint. This gives rise to a smooth intensity distribution in the focal plane of the CPT.

The concentration characteristics of a CPT are given by: i) the value of  $I_0(y)$ , ii) the width of the focal plane over which a nonzero intensity is obtained, this will naturally be  $L_k$ ; and iii) receiver intercept fraction. The first two are easily determined from the above analysis. The third one, the receiver intercept fraction, is defined as the fraction  $F$  of the total concentrated flux intercepted by a target of given width  $y_t$ , centrally located in the focal plane

$$F = \frac{\left[ \int_{-y_t/2}^{y_t/2} I(y) dy \right]}{pq_s W}, \quad (7)$$

where  $I(y)$  is the intensity distribution in the receiver plane which has been determined above, and  $W$  is the concentrator width given by

$$W = d \left( 1 + \sum_{n=1}^k 2 \cos \Psi_n \right). \quad (8)$$

The quantity  $F$  is significant in that it gives the concentration efficiency as  $pF$  and the concentration ratio as  $(pWF/y)$  which both are useful design parameters.

## Results and discussions

To evaluate the constructional parameters and concentration characteristics of a CPT with the help of the above mentioned ray-optical model, it is necessary to know the coordinates of the end-points of various mirror elements on the base of parabolic shape. Analytical relations to obtain these values turn out to be tedious and hence numerical iterative techniques based on lens designer's ray tracing methodology are used instead. Thus, the analysis formulated in the present paper gives the characteristics of a CPT at the level of design stage ray-optical assessments. Figure 2 shows the variation of  $L_k$  and  $I_0(y)$ , evaluated from (1), (2), (3), and (5),

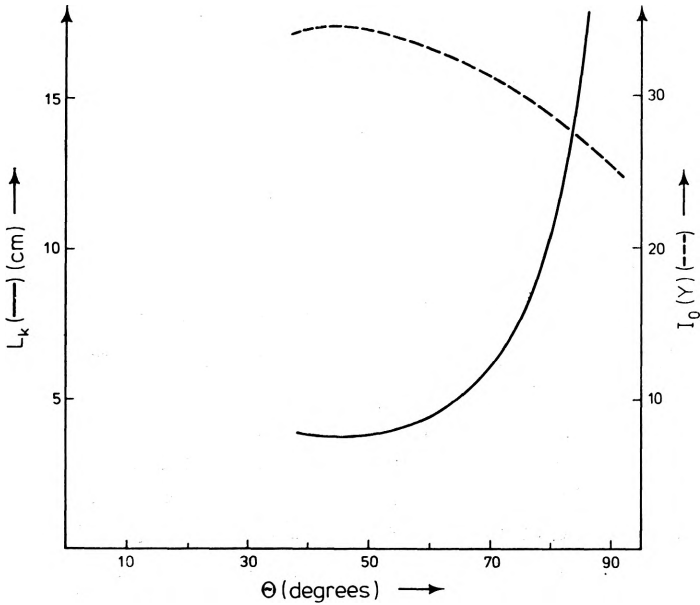


Fig. 2. Variation of  $L_k$  and  $I_0(y)$  with  $\Theta$ ;  $d = 0.02$  meters,  $D = 1.00$  meter

with rim angle for  $D = 1$  meter and  $d = 2$  cm. It may be seen that both these parameters take extreme values at a rim angle of  $45^\circ$ , but, whereas  $L_k$  shows a step rises,  $I_0(y)$  shows only a gradual decrease with increasing rim angles. This implies that the size of the region of the focal plane with nonzero intensity increases without much effect on the local concentration at the central solar image.

Figure 3 is a graphical representation of several other constructional and concentration characteristics of a CPT. The values of  $\Psi_n$ ,  $L_n$ , and  $CI_n$  have been shown here for various constituent mirror elements of a CPT. The behaviour of  $\Psi_n$  is here

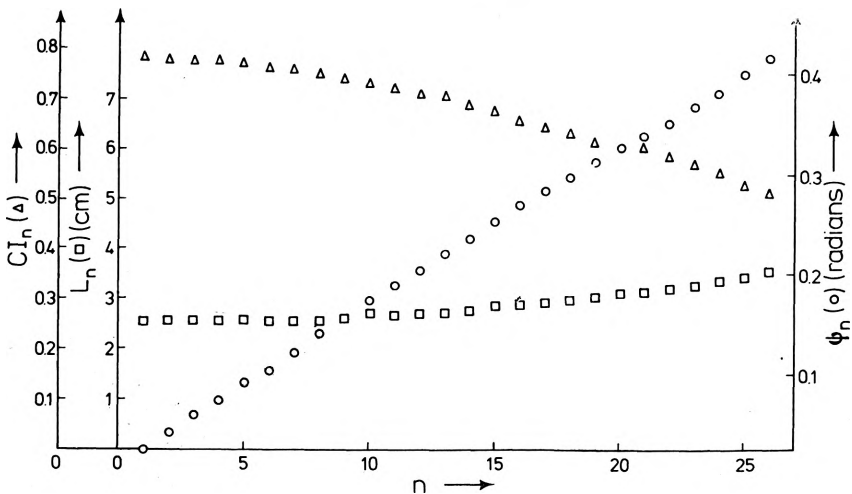


Fig. 3.  $\Psi_n$ ,  $L_n$ , and  $CI_n$  for various mirror elements;  $d = 0.02$  meters,  $\Theta = 45^\circ$ ,  $D = 1.00$  meter

constrained by the choice of a parabola for the base curve of the concentrator. That the variation of  $\Psi_n$  will be linear with the position of the element is also clear from the fact that, for limitingly small sizes of the mirror elements,  $\Psi_n$  is simply given by the slope of the tangent to the parabola at that point. The change in  $L_n$  implies again that although the region of nonzero intensity outside the central solar image, formed by the axial mirror element, increases, the contribution of the extra-axial elements to the total concentrated flux on the central solar image is low. This effect is reflected further in intensity distribution curves shown in fig. 4, where the

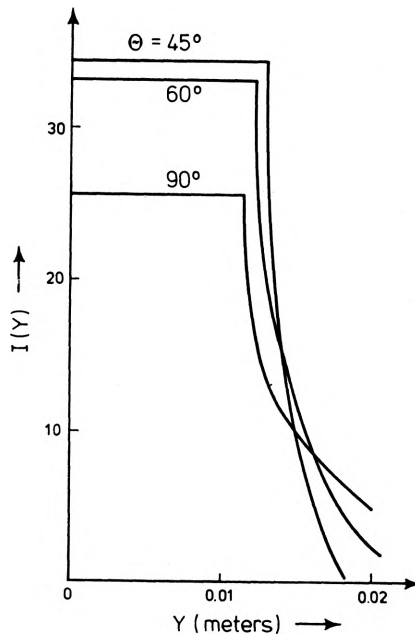


Fig. 4. Intensity distribution in the receiver plane;  $d = 0.02$  meters,  $D = 1.00$  meter

distributions are seen to have extended tails for higher rim angles. The variation of the receiver intercept fraction,  $F$  vs.  $y_t$ , curves with rim angle are plotted in fig. 5. This is important in those applications of concentrator, where one is interested in the total energy collected by the receiver as it leads to an optimum choice of the rim angle and receiver size.

### Concluding remarks

A simple design stage ray-optical assessment of a typical CPT has been given above providing theoretical limits for the concentrator-receiver sizes which are expected to form a basis for the preliminary design of plant subsystems and relative cost performance trade-off studies. Further analysis, on which work is progressing at our Institute, also may be expected to include effects of other parameters, such as the spatial and temporal spectra of the solar radiation, on the optical performance of a CPT.

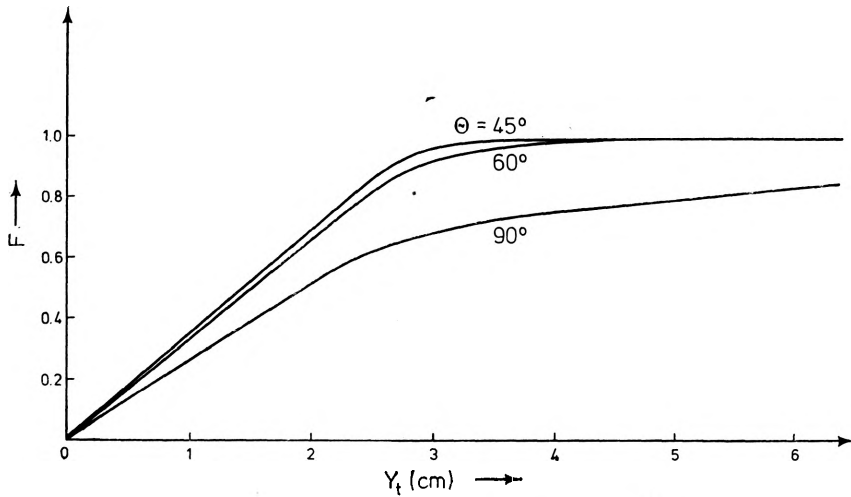


Fig. 5. Receiver's intercept fraction  $F$ ;  $d = 0.02$  meter,  $D = 1.00$  meter

*Acknowledgement* — The authors are greatly indebted to Professor M. Sodha for constant encouragement.

## References

- [1] EVANS D. L., *Solar Energy* **19** (1977), 379–385.
- [2] McDERMIT J. H., HORTON T. E., *Optical design of solar concentrators*; presented at 2nd AIAA/ASME Thermophysics and Heat Transfer Conf., Palo Alto, California 1978.
- [3] GIUTRONICH J. E., *Solar Energy* **9** (1963), 162–166.
- [4] SHAPIRO M. M., *Solar Energy* **19** (1977), 211–213.
- [5] COSBY R. M., *Concentration characteristics of Fresnel solar strip reflection concentrator*, NASA-CR-120336, 1974.

*Received, May 3, 1979*